

Synthesis, crystal structure and spin-density-wave anomaly of the iron arsenide-fluoride SrFeAsF

MARCUS TEGEL¹, SEBASTIAN JOHANSSON¹, VERONIKA WEISS¹, INGA SCHELLENBERG², WILFRIED HERMES², RAINER PÖTTGEN² and DIRK JOHRENDT¹

¹ *Department Chemie und Biochemie, Ludwig-Maximilians-Universität München, Butenandtstrasse 5-13 (Haus D), 81377 München, Germany*

² *Institut für Anorganische und Analytische Chemie, Universität Münster, Corrensstrasse 30, D-48149 Münster, Germany*

PACS 74.10.+v – Superconductivity; Occurrence, potential candidates
 PACS 74.70.Dd – Superconductivity; Ternary, quaternary, and multinary compounds
 PACS 71.27.+a – Strongly correlated electron systems
 PACS 75.30.Fv – Spin-density waves
 PACS 61.50.Ks – Crystallographic aspects of phase transformations
 PACS 61.05.cp – X-ray diffraction
 PACS 33.45.+x – Mössbauer spectra

Abstract. - The new quaternary iron arsenide-fluoride SrFeAsF with the tetragonal ZrCuSiAs-type structure was synthesized and the crystal structure was determined by X-ray powder diffraction ($P4/nmm$, $a = 399.30(1)$, $c = 895.46(1)$ pm). SrFeAsF undergoes a structural and magnetic phase transition at 175 K, accompanied by strong anomalies in the specific heat, electrical resistance and magnetic susceptibility. In the course of this transition, the space group symmetry changes from tetragonal ($P4/nmm$) to orthorhombic ($Cmme$). ⁵⁷Fe Mössbauer spectroscopy experiments show a single signal at room temperature at an isomer shift of 0.30(1) mm/s and magnetic hyperfine-field splitting below the phase transition temperature. Our results clearly show that SrFeAsF exhibits a spin density wave (SDW) anomaly at 175 K very similar to LaFeAsO, the parent compound of the iron arsenide-oxide superconductors and thus SrFeAsF may serve as a further parent compound for oxygen-free iron arsenide superconductors.

Introduction. – The discovery of superconductivity in doped iron-arsenides with ZrCuSiAs-type [1] and ThCr₂Si₂-type [2] structures with critical temperatures up to 55 K [3, 4] have heralded a new age in superconductivity research. The parent compounds of these superconductors are built up by alternating layers of (FeAs)⁻ and (LaO)⁺ or $\frac{1}{2}$ Ba²⁺, respectively. The crystal structure of LaFeAsO is depicted in Figure 1. Structural phase transitions from tetragonal to orthorhombic lattice symmetry occur prior to antiferromagnetic ordering [5, 6] and both can be suppressed by electron or hole doping, which also induces superconductivity. At first it was believed that this suppression is a prerequisite to superconductivity, but recent results strongly suggest that superconductivity coexists with the orthorhombic and magnetic phases for low doping at least in SmFeAsO and BaFe₂As₂ [7–9]. Beyond strong efforts to shed light on the properties and mecha-

nism of superconductivity, the search for further materials with possibly higher critical temperatures is still going on.

In this letter, we report on the iron arsenide fluoride SrFeAsF with tetragonal ZrCuSiAs-type structure, where the (LaO)⁺ layers of LaFeAsO are replaced for (SrF)⁺ layers. Our results clearly reveal that SrFeAsF exhibits a spin-density wave anomaly at 175 K as typical for these compounds and therefore may serve as a new parent compound for high- T_c superconductors.

Experimental. – SrFeAsF was synthesized by heating a mixture of strontium fluoride, distilled strontium metal, H₂-reduced iron-powder and sublimed arsenic at a ratio of 1:1:2:2 in a sealed niobium tube under an atmosphere of purified argon. The mixture was heated to 1173 K at a rate of 50 K/h, kept at this temperature for 40 h and cooled down to room temperature. The product was homogenized in an agate mortar, pressed into pellets and

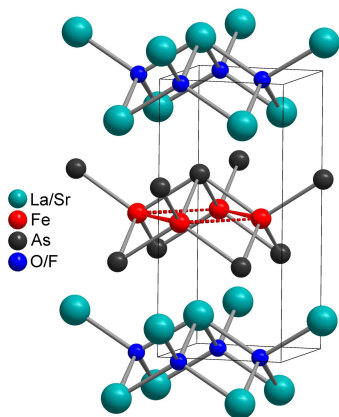


Fig. 1: Crystal structure of LaFeAsO and SrFeAsF.

sintered at 1273 K for 48 h. The obtained black crystalline powder of SrFeAsF is stable in air.

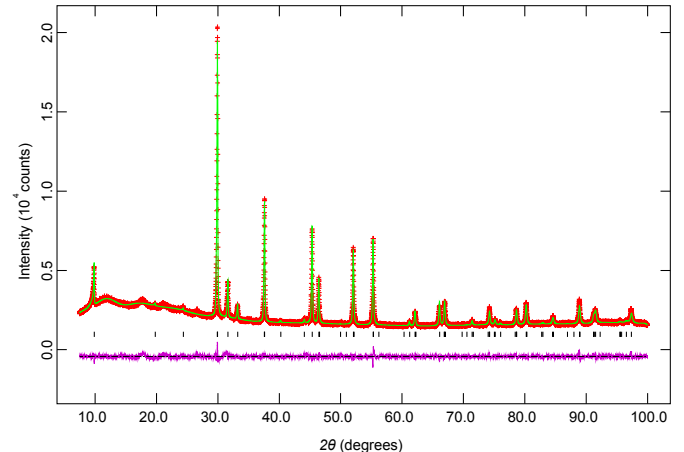
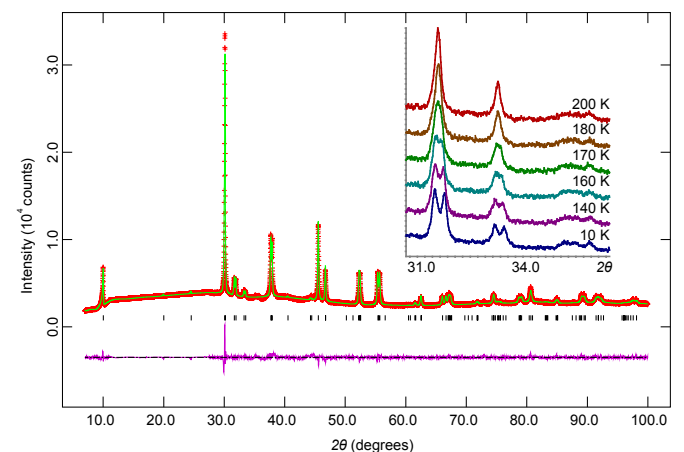
Phase purity was checked by X-ray powder diffraction on a Huber G670 Guinier imaging plate diffractometer ($\text{Cu-K}\alpha_1$ radiation, Ge-111 monochromator), equipped with a closed-cycle cryostat. Rietveld refinements of SrFeAsF were performed with the GSAS package [10] using Thompson-Cox-Hastings functions with asymmetry corrections as reflection profiles. [11] To obtain lattice parameter changes of highest possible accuracy, asymmetry parameters as well as the gaussian parameters U and V were refined at 10 K and held constant for all other temperatures.

A $^{57}\text{Co/Rh}$ source was available for ^{57}Fe Mössbauer spectroscopy investigations. The SrFeAsF sample was placed in a thin-walled PVC container. The measurement was run in the usual transmission geometry at temperatures between 4.2 and 298 K. The source was kept at room temperature. The total counting time was approximately one day per spectrum. Fitting of the spectra was performed with the NORMOS-90 program system. [12]

Heat capacity measurements between 2.1 and 305 K were carried out on a Quantum Design Physical Property Measurement System (PPMS). The sample was fixed to the platform of a pre-calibrated heat capacity puck using Apiezon N grease. The magnetic susceptibility was measured with a SQUID magnetometer (MPMS-XL5, Quantum Design Inc.) at 0.1 T.

Results and Discussion. – Figure 2 shows the X-ray powder pattern of SrFeAsF, which was completely fitted with a single tetragonal ZrCuSiAs-type SrFeAsF phase. Impurities are, if at all, less than 1 %. In order to check for a structural phase transition, we have subsequently recorded patterns between 297 and 10 K. Several reflections broaden below 185 K and clearly split with further decreasing temperature. Patterns below 185 K were indexed with an orthorhombic C -centered unit cell ($a_{ortho} = \sqrt{2} \cdot a_{tetra} - \delta$; $b_{ortho} = \sqrt{2} \cdot b_{tetra} + \delta$; $c_{ortho} \approx c_{tetra}$; $\delta \approx$

2.2 pm). The low temperature data could be refined in the space group $Cmme$. Figure 3 shows the Rietveld fit of the data at 10 K and the continuous transition of the (2 0 0) and (2 0 1) reflections in the inset.

Fig. 2: (Color online) X-ray powder pattern (+) and Rietveld fit (-) of SrFeAsF at 297 K (space group $P4/nmm$).Fig. 3: (Color online) X-ray powder pattern (+) and Rietveld fit (-) of SrFeAsF at 10 K (space group $Cmme$). For more accurate results, the range between 11 and 27.5 2θ was excluded from the Rietveld refinement. Inset: Splitting of the (2 0 0) and (2 0 1) reflections.

The variation of the lattice parameters and the temperature dependence of the order parameter $P = \frac{a-b}{a+b}$ is depicted in Figure 4. The a lattice parameter in the tetragonal structure has been multiplied by $\sqrt{2}$ for comparison. We have found no signs of abrupt splitting of any reflections and also lattice parameters on cooling, but rather a continuous broadening. The space group $Cmme$ is a subgroup of $P4/nmm$ and therefore a second order phase transition is in agreement with our data. In terms of group theory, this transition is *translationengleich* with index 2 ($P4/nmm \rightarrow Cmme$). Crystallographic data of SrFeAsF are summarized in Table 1. The main effect of

the phase transition appears in the Fe–Fe distances, where four equal bonds of 282.3 pm length split into two pairs of 283.0 and 280.7 pm length, respectively. This supports the idea, that the Fe–Fe interactions are strongly correlated with the SDW anomaly and may play a certain role for the properties of SrFeAsF.

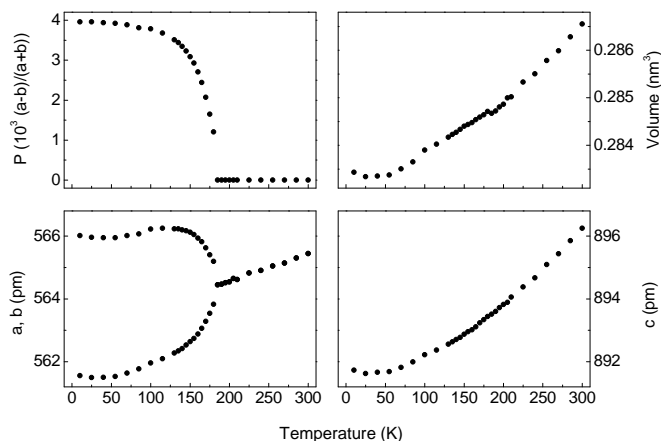


Fig. 4: Variation of the lattice parameters with temperature and order parameter $P = \frac{a-b}{a+b}$. The temperature dependence of the order parameter does not follow a simple power law. Values a and b for the tetragonal phase above 180 K are multiplied by $\sqrt{2}$ for comparability. Error bars are within data points.

In order to check if the structural transition of SrFeAsF is connected with magnetic ordering and thus consistent with a SDW anomaly, we have recorded ^{57}Fe Mössbauer spectra at various temperatures, which are shown in Figure 5 together with transmission integral fits. The corresponding fitting parameters are listed in Table 2. In agreement with the crystal structure, at room temperature we observed a single signal at an isomer shift of $\delta = 0.33(1)$ mm/s and an experimental line width $\Gamma = 0.30(1)$ mm/s subject to quadrupole splitting of $\Delta E_Q = -0.11(1)$ mm/s. The non-cubic site symmetry of the iron atoms is reflected in the quadrupole splitting value. These parameters compare well with the recently reported ^{57}Fe data for LaFeAsO [13,14], LaFePO [15], SrFe₂As₂ [16], and BaFe₂As₂. [5] Below the SDW transition temperature, we observed line broadening of the signal followed by hyperfine field splitting due to the onset of magnetic order. As it can be clearly seen, there is a large evolution of the shape of the spectra with decreasing temperature. In the magnetically ordered state, the ^{57}Fe Mössbauer spectra of the SrFeAsF sample show significant differences when compared to the related systems SrFe₂As₂ [16] and BaFe₂As₂. [5] It was not possible to reliably analyze the data with only one magnetically split component below the SDW transition temperature. However, the spectra could be effectively fitted assuming a distribution of hyperfine magnetic fields (multi-component analysis), an approach similar to the WIVEL and MØRUP method. [17] The probability distribution curves $P(B_{hf})$ as a function of tem-

perature are shown in Figure 5. As a test for the program system we have also fitted the BaFe₂As₂ data from ref. [5] with the same algorithm. Since BaFe₂As₂ shows almost full hyperfine field splitting at 77 K, the distribution curve shows a single sharp contribution around 5 T. For SrFeAsF we observed a shift of the field components towards higher hyperfine fields with decreasing temperature. During numerical analysis, special attention was paid to the line width and quadrupole splitting parameters. These values were held constant at the values listed in Table 2. The magnitudes of the average hyperfine fields obtained from the data analysis are also listed in Table 2.

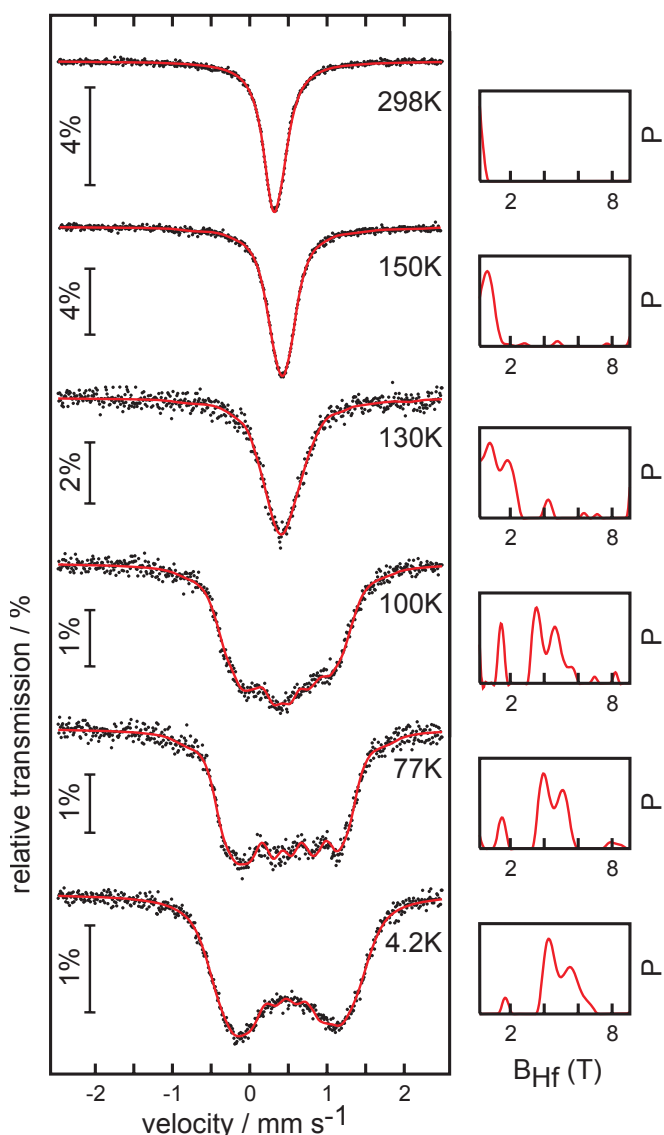


Fig. 5: Experimental and simulated ^{57}Fe Mössbauer spectra of SrFeAsF. The temperature evolution of the field distribution functions, $P(B_{hf})$, obtained from computer fits at various temperatures are presented at the right-hand parts of the spectra. For details see text.

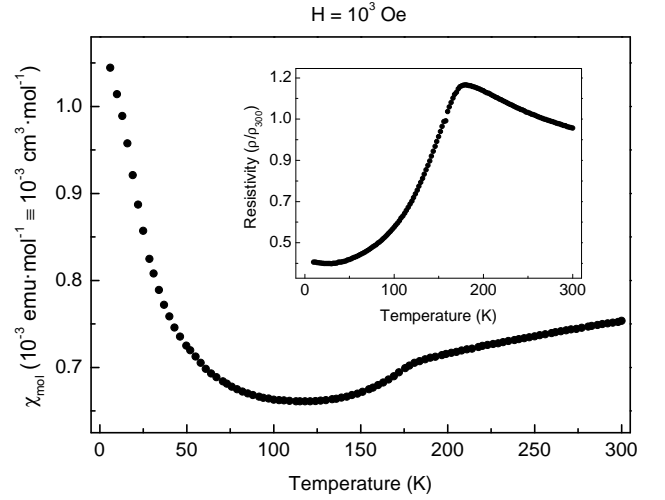
Table 1: Crystallographic data of SrFeAsF.

Temperature (K)	297	10
Space group	$P4/nmm$	$Cmme$
a (pm)	399.30(1)	561.55(1)
b (pm)	$= a$	566.02(1)
c (pm)	895.46(1)	891.73(2)
V (nm ³)	0.14277(1)	0.28343(1)
Z	2	4
data points	9250	7649
reflections	66	97
atomic variables	6	6
profile variables	4	4
d range	0.992 – 8.955	0.988 – 8.917
R_P, wR_P	0.0311, 0.0408	0.0385, 0.0611
$R(F^2), \chi^2$	0.0408, 1.771	0.0552, 2.860
Atomic parameters:		
Sr	$2c (\frac{1}{4}, \frac{1}{4}, z)$ $z = 0.1598(2)$ $U_{iso} = 185(9)$	$4g (0, \frac{1}{4}, z)$ $z = 0.1635(2)$ $U_{iso} = 227(12)$
Fe	$2b (\frac{3}{2}, \frac{1}{4}, \frac{1}{2})$ $U_{iso} = 75(8)$	$4b (\frac{1}{4}, 0, \frac{1}{2})$ $U_{iso} = 142(12)$
As	$2c (\frac{1}{4}, \frac{1}{4}, z)$ $z = 0.6527(2)$ $U_{iso} = 46(8)$	$4g (0, \frac{1}{4}, z)$ $z = 0.6494(2)$ $U_{iso} = 60(11)$
F	$2a (\frac{3}{4}, \frac{1}{4}, 0)$ $U_{iso} = 210(26)$	$4a (\frac{1}{4}, 0, 0)$ $U_{iso} = 114(33)$
Bond lengths (pm):		
Sr–F	245.7(1)×4	247.0(1)×4
Fe–As	242.0(1)×4	239.7(1)×4
Fe–Fe	282.3(1)×4	283.0(1)×2, 280.7(1)×2
Bond angles (deg):		
As–Fe–As	111.2(1)×2 108.6(1)×4	112.5(1)×2, 108.3(1)×2, 107.7(1)×2
Sr–F–Sr	108.7(1)×2 109.8(1)×4	110.7(1)×2, 110.1(1)×2, 107.6(1)×2

Table 2: Fitting parameters of ⁵⁷Fe Mössbauer spectra of SrFeAsF at different temperatures. δ : isomer shift; ΔE_Q : electric quadrupole splitting parameter; Γ : experimental line width; B_{hf} : average hyperfine field at the iron nuclei (for details see text). Parameters marked with an asterisk were held constant during the fitting procedure. Γ , δ and ΔE_Q are given in ($mm \cdot s^{-1}$).

T (K)	Γ	δ	ΔE_Q	B_{hf}
298	0.30*	0.32*	0.08(1)	–
130	0.26*	0.40*	-0.01(1)	1.78(1)
100	0.26*	0.45*	0.03(1)	3.64(1)
77	0.26*	0.45*	0.32(1)	4.08(1)
4.2	0.28*	0.40*	0.20(1)	4.84(3)

So far, our results clearly prove a structural distortion in SrFeAsF, connected with magnetic ordering. The nature of this effect is completely analogous to that in LaFeAsO. [18] The transition is driven by a spin density (SDW) instability within the iron layers and therefore causes anomalies in the electrical resistivity and magnetic susceptibility. We have measured these properties of SrFeAsF and found the same behavior. The temperature dependencies of the magnetic susceptibility and dc electrical resistance are depicted in Figure 6. SrFeAsF shows a relatively high resistance at room temperature. At 175 K, the resistance drops abruptly and then decreases slowly with lower temperatures. SrFeAsF shows a weak and only slightly temperature-dependent paramagnetism, as typical for a Pauli-paramagnetic metal. Below 175 K, χ drops at first but it increases again below 115 K.


Figure 6: Magnetic susceptibility of SrFeAsF measured at 0.1 T. Inset: dc electrical resistance ($I = 100 \mu A$).

The specific heat data of SrFeAsF are shown in Figure 7. At room temperature the specific heat capacity reaches the value of approximately 100 J/mol·K, in agreement with the law of Dulong and Petit. The phase transition of SrFeAsF becomes noticeable by an anomaly, which can be seen in Figure 7. The transition temperature has been determined as the inflection point of the anomaly (on the right-hand side). Thus, the C_p data are in line with the resistivity, X-ray powder diffraction, and Mössbauer spectroscopic data. In the low temperature region, the specific heat is of the form $C_p = \gamma T + \beta T^3$, where γ is the electronic contribution and β is the lattice contribution. The Debye temperature Θ_D can be estimated from the equation $\beta = (12\pi^4 n k_B)/(5\Theta_D^3)$, where k_B is the Boltzmann constant and n is the number of atoms per formula unit. From the plot of C_p/T vs. T^2 in the temperature range 4–10 K we found $\gamma = 1.5(2) \text{ mJ}\cdot\text{K}^{-2}\cdot\text{mol}^{-1}$, $\beta = 0.2(1) \text{ mJ}\cdot\text{K}^{-4}\cdot\text{mol}^{-1}$, and $\Theta_D = 339(1) \text{ K}$.

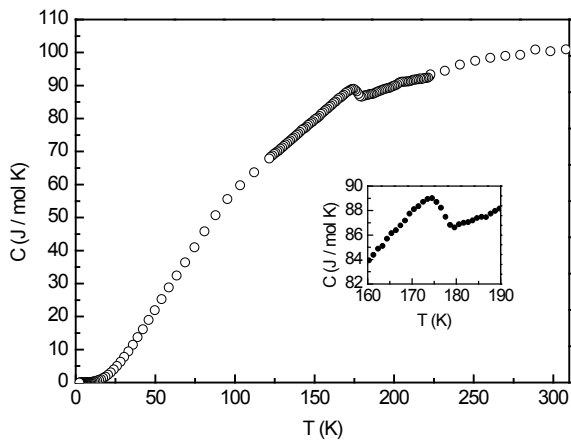


Fig. 7: Heat capacity (C_P) vs. temperature for SrFeAsF. The inset highlights the features between 160 and 190 K.

Summary. — We have synthesized the quaternary iron arsenide fluoride SrFeAsF, which crystallizes in the ZrCuSiAs-type structure. The properties of SrFeAsF are very similar to LaFeAsO, the parent compound of the recently discovered superconductors. Both materials are poor metals at room temperature and undergo second order structural and magnetic phase transitions. The ^{57}Fe Mössbauer data of SrFeAsF show hyperfine field splitting, which indicates antiferromagnetic ordering occurring below the structural transition temperature. Consequently, SrFeAsF exhibits the same SDW anomaly at 175 K as LaFeAsO at 150 K. Since this SDW instability is known to be an important prerequisite for high- T_C superconductivity in iron arsenides, our results strongly suggest that SrFeAsF can serve as a parent compound for a new, oxygen-free class of iron arsenide superconductors with ZrCuSiAs-type structure. It is highly probable that superconductivity in SrFeAsF can be induced either by electron or hole doping.

While we were finalizing our manuscript, we took notice of a recently published article on Co-doped CaFeAsF. [20] Therein, superconductivity was found below 22 K, which renders this new class of materials a very promising candidate for superconductors with high critical temperatures.

This work was financially supported by the DFG.

REFERENCES

- [1] KAMIHARA Y., WATANABE T., HIRANO M. and HOSONO H., *J. Am. Chem. Soc.*, **130** (2008) 3296.
- [2] ROTTER M., TEGEL M. and JOHRENDT D., *Phys. Rev. Lett.*, **101** (2008) 107006.
- [3] JOHRENDT D. and PÖTTGEN R., *Angew. Chem. Int. Ed.*, **47** (2008) 4782.
- [4] REN Z.-A. ET AL., *Chin. Phys. Lett.*, **25** (2008) 2215.
- [5] ROTTER M., TEGEL M., SCHELLENBERG M., HERMES W., PÖTTGEN R. and JOHRENDT D., *Phys. Rev. B*, **78** (2008) 020503(R).
- [6] C. DE LA CRUZ ET AL., *Nature*, **453** (2008) 899.
- [7] MARGADONNA S., TAKABAYASHI Y., McDONALD M. T., BRUNELLI M., WU G., LIU R. H., CHEN X. H., PRASSIDES K., *arXiv:0806.3962* 2008.
- [8] ROTTER M., PANGERL M., TEGEL M. and JOHRENDT D., *Angew. Chem. Int. Ed.*, **47** (2008) 7949.
- [9] CHEN H., REN Y., QIU Y., BAO W., LIU R. H., WU G., WU T., XIE Y. L., WANG X. F., HUANG Q., CHEN X. H., *arXiv:0807.3950*, 2008
- [10] LARSON A. C. and V. DREELE R. B., *General Structure Analysis System* 2000.
- [11] FINGER L. W., COX D. E. and JEPHCOAT A. P., *J. Appl. Crystallogr.*, **20** (1987) 79.
- [12] BRAND R. A., *Normos Mössbauer fitting Program*, (Universität Duisburg) 2002.
- [13] KITAO S., KOBAYASHI Y., HIGASHITANGUCHI S., SAITO M., KAMIHARA Y., HIRANO M., MITSUI T., HOSONO H. and SETO M., *arXiv:0805.0041*, 2008.
- [14] KLAUSS H.-H., LUETKENS H., KLINGELER R., HESS C., LITTERST F. J., KRAKEN M., KORSHUNOV M. M., EREMIN I., DRECHSLER S.-L., KHASANOV R., AMATO A., HAMANN-BORRERO J., LEPS N., KONDRAT A., BEHR G., WERNER J. and BÜCHNER B., *Phys. Rev. Lett.*, **101** (2008) 077005.
- [15] TEGEL M., SCHELLENBERG I., PÖTTGEN R. and JOHRENDT D., *Z. Naturforsch. B*, **63b** (2008) 1057.
- [16] TEGEL M., ROTTER M., WEISS V., SCHAPPACHER F. M., PÖTTGEN R. and JOHRENDT D., *J. Phys.: Condens. Matter*, **20** (2008) 452201.
- [17] WIVEL C. and MØRUP S., *J. Phys. E*, **14** (1981) 605.
- [18] NOMURA T., KIM S. W., KAMIHARA Y., HIRANO M., SUSHKO P. V., KATO K., TAKATA M., SHLUGER A. L., and HOSONO H., *arXiv:0804.3569*, 2008.
- [19] DONG J., ZHANG H. J., XU G., LI Z., LI G., HU W. Z., WU D., CHEN G. F., DAI X., LUO J. L., FANG Z. and WANG N. L., *Europhysics Letters*, **83** (2008) 27006.
- [20] MATSUISHI S., YASUNORI I., NOMURA T., YANAGI H., HIRANO M. and HOSONO H., *J. Am. Chem. Soc.*, (2008) in press.